Am J Cancer Res 2020;10(3):1012-1025
www.ajcr.us /ISSN:2156-6976/ajcr0104712

Original Article

METTL3 enhances cell adhesion through stabilizing integrin β1 mRNA via an m6A-HuR-dependent mechanism in prostatic carcinoma

Ermao Li[1*], Bo Wei[1*], Xiaolan Wang[3], Ran Kang[2]

[1]Research Lab for Clinical & Translational Medicine, Medical school, University of South China, Hengyang, Hunan, China; [2]Department of Urology, [3]Reproductive Center of Medicine, The First Affiliated Hospital of University of South China, Hengyang, Hunan, China. [*]Equal contributors.

Received November 10, 2019; Accepted January 13, 2020; Epub March 1, 2020; Published March 15, 2020

Abstract: Bone metastasis is the major cause of morbidity and mortality in patients with prostate cancer (PCa). However, the underlying mechanism of bone-specific metastasis remain vague. Recently, with the deep research of N6-methyladenine (m6A) mRNA methylation, many studies directly focus on the role of m6A modification in human diseases, especially in cancers. Here we found that methyltransferase-like 3 (METTL3) expression is higher in PCa than in normal prostate tissues, especially in PCa with bone metastasis. High METTL3 expression was positively correlated with advanced progression and a poor prognosis of PCa. Functional assays demonstrated that METTL3 regulates the expression of Integrin β1 (ITGB1) through m6A-HuR-dependent mechanism, which affects the binding of ITGB1 to Collagen I and tumor cell motility, so as to promote the bone metastasis of PCa. The findings of this study reveal a novel mechanism of PCa osteotropism and suggest METTL3 as a therapeutic target for PCa bone metastasis.

Keywords: METTL3, prostate cancer, ITGB1, cell adhesion, HuR

Introduction

Prostate cancer (PCa) is the most commonly diagnosed form of cancer and the second leading cause of cancer-related deaths among men worldwide [1], in which metastasis to the bone is the main cause of death [2]. More than 60% of advanced PCa patients are found bone metastasis, and an autopsy found evidence of bone metastases in more than 90% of patients diagnosed with PCa. The overall 5-year survival of patients with localized PCa was approximates 100%, however, less than 31% for patients in whom bone metastases occurred [3]. These patients with bone metastasis had serious complications, such as ostealgia, spinal cord compression and pathological fracture [4], seriously affected the life quality and survival rate of patients. Therefore, a better understanding of the molecular mechanism of cancer metastasis is benefit to treat PCa with bone metastases.

In more recent years, epigenetic modification to RNA species have received attention in many countries and science. More than 100 types of chemical modifications have been identified in RNAs so far, which are widely distributed on messenger RNAs (mRNAs), transfer RNAs (tRNAs), ribosomal RNAs (rRNAs) and other non-coding RNAs [5, 6]. N6-methyladenosine (m6A) is one of the most abundant post-transcriptional modifications identified in RNAs [7]. Analogous to DNA and histone, it is a reversible methylation modification via regulation of m6A modification methyltransferase, demethylase and proteins that preferentially recognize m6A modification as “writers”, “erasers” and “readers”, respectively [8]. m6A participates in regulation of various aspects of mRNA metabolism including RNA processing [9], RNA transporting from nucleus to cytoplasm [10], RNA translation [11], and RNA decay [12]. m6A methylation has been found to have an impact on cancer stem cell pluripotency, cancer cell proliferation and

aggression through various mechanisms [13]. Despite m6A RNA methylation can metastatic potential of many tumours, including hepatocellular carcinoma, colorectal carcinoma and pancreatic cancer et al. [14-16], the functional mechanisms of m6A in PCa bone metastasis are still not well understood.

Here, we first demonstrated the function of METTL3 in facilitating PCa bone metastasis by inducing ITGB1/Collagen I-associated pathways through affecting mRNA m6A modification, in an attempt to elucidate the potential mechanism of PCa organotropic metastasis.

Materials and methods

Patients and tissue specimens

A total of 15 localized PCa tissues, 15 PCa with BM and corresponding adjacent tissues were retrieved from consecutive PCa patients who underwent radical prostatectomy at the First Affiliated Hospital of Guangzhou Medical University between January 2008 and December 2013. The study was approved by the human study ethics committees at our Hospital, and all cases gave the informed consent.

Cell lines and cell culture

The human PCa cells PC3 and LNCaP were obtained from the ATCC. LNCaP were maintained in DMEM basic (Gbico) supplemented with 10% fetal bovine serum (Gbico) and a 1% penicillin and streptomycin combination. PC3 were maintained in 1640 (Gbico) supplemented with 10% fetal bovine serum (Gbico) and a 1% penicillin and streptomycin combination. All cells grew in standard cell culture conditions (5% CO_2, 95% humidity) at 37°C.

Plasmids and transfections

The shRNAs targeting METTL3 and ITGB1 were purchased from GenePharma (Shanghai, China) and were transfected with Lipofectamine2000 (Invitrogen, Carlsbad, CA). Those shRNA sequences are summarized in Table S1. The METTL3 and HuR CDS obtained by PCR product (PCR primer sequence as followed in Table S2) was ligated into the pCDNA3.1 (+) vector. The stable cell lines PC3-shMETTL3 and LNCaP-METTL3 were established as described previously [17]. ITGB1-CDS-WT (wild-type CDS of ITGB1), ITGB1-CDS-Mut (mutant CDS of ITGB1, m6A was replaced by T in the m6A motifs), ITGB1-5'UTR-WT (wild-type 5'UTR of ITGB1), ITGB1-5'UTR-Mut (mutant 5'UTR of ITGB1, m6A was replaced by T in the m6A motifs) were ligated into the pMIR-REPORT and pGL3-Basic vector, respectively. Control pRL-sv40 plasmid was purchased from Promega.

Immunohistochemical analysis

Expression pattern and subcellular localization of METTL3 protein in clinical PCa tissues were detected by immunohistochemistry and the immunoreactivity scores (IRS) of METTL3 were calculated according to the protocol previously described [17].

In vitro cell adhesion assay

Triplicate wells on a 96-well cell culture plate were coated with 1 μg/cm^2 type I Collagen (BD Biosciences) or a single layer of BMECs for overnight at 37°C, washing the plate three times with serum-free medium. The plates were blocked with 1% BSA in DMEM for 2 hours at 37°C. A total of 2 × 10^4 cells were seeded in the blocked 96-well plate for 15-30 min, then the supernatant and the non-adhesion cells were removed with PBS. 100 μl DMEM-free medium with 10 μl of MTS added to the each plates and the cells were incubated for another 4 hours at 37°C. The absorbance of the solution was measured with a 490 nm filter.

Quantitative reverse transcription-PCR

Total RNA from cells was isolated with TRIzol (Invitrogen) as described previously [17]. Selected sequences of the sense and antisense primers were used for the amplification (Table S2). All values were normalized for the GAPDH expression levels. Relative quantification of mRNA levels was determined by $2^{-\Delta\Delta CT}$ method.

Western blotting

Western blot analysis was conducted as previously described by our laboratory [17]. The primary antibodies used included antibodies against METTL3 (ab#195352, Abcam), HuR (ab#200342, Abcam), ITGB1 (ab#24693, Abcam), GAPDH (ab#8245, Abcam). The secondary antibodies were anti-mouse and anti-rabbit

IgG conjugated with HRP (ab#136815, ab# 136817, Abcam).

m6A dot blot assay

Isolate mRNA from total RNA using the Dynabeads® mRNA Purification Kit following the manufacturer's instructions. Denature the serially diluted mRNA at 95°C to disrupt secondary structures in a heat block for 3 min, chill on ice immediately after denaturation; Crosslink spotted mRNA to membrane in a Stratalinker 2400 UV Crosslinker twice. Incubate the membrane in blocking buffer for 1 h at room temperature with gentle shaking. Incubate the membrane with anti-m6A antibody overnight at 4°C with gentle shaking, then incubate the membrane with goat anti-rabbit IgG-HRP for 1 h at room temperature. Wrap the membrane in plastic wrap and expose with Hyperfilm ECL for a proper exposure period.

Dual-luciferase reporter assay

2×10^4 cells per well were plated in 96-well plates and transfected with 100 ng of ITGB1-luciferase plasmid. To normalize transfection efficiency, the cells were co-transfected with 10 ng of pRL-CMV (Renilla luciferase). After 48 h, the luciferase activity was measured using the Dual-Luciferase Assay kit (Promega, Madison, WI, USA). Three independent experiments were performed, and the calculated means and standard deviations are presented.

Gene-specific m6A qPCR

Total RNAs were first extracted from LNCaP and PC3 cells. Chemically fragmented RNA was incubated with m6A antibody for immunoprecipitation according to the standard protocol of the Magna methylated RNA immune-precipitation (MeRIP) m6A Kit (Merck Millipore). Enrichment of m6A containing mRNA was then analyzed either through quantitative reverse-transcription polymerase chain reaction (qRT-PCR).

RNA Binding Protein Immunoprecipitation (RIP)

RIP was conducted with the RIP™ RNA-Binding Protein Immunoprecipitation Kit (Millipore) according to the manufacturer's instructions. Briefly, magnetic beads coated with 5 μg of specific antibodies against METTL3 (ab#1953-52, Abcam) were incubated with prepared cell lysates overnight at 4°C. Then, the RNA-protein complexes were washed 6 times and incubated with proteinase K digestion buffer. RNA was finally extracted by phenol-chloroform RNA extraction methods. The relative interaction between METTL3 and ITGB1 transcripts was determined by qPCR and normalized to the input.

RNA stability assay

Actinomycin D (A9415, Sigma-Aldrich) was added to PCa cells at 5 mg/ml to assess RNA stability. After incubation for indicated time points, the cells were collected and RNA samples were extracted for reverse transcription and qPCR. mRNA transcription was inhibited with Actinomycin D and the degradation rate of RNA (K decay) was estimated by following equation: $ln(C/C_0) = K_{decay}t$.

C_0 is the concentration of mRNA at time 0, t is the transcription inhibition time, and C is the mRNA concentration at the time t. Thus the K decay can be derived by the exponential decay fitting of C/C_0 versus time t. The half-time (t 1/2), which means C/C_0 = 50%/100% = 1/2, can be calculated by the following equation: $ln(1/2) = -K_{decay}t_{1/2}$.

In vivo metastasis assay

Twenty 5-week-old male SCID mice were supplied by the Experimental Animal Center of Guangdong Province, China. The animals were maintained in a special pathogen free facility. All the mice were randomly divided into five groups of four mice each, including PC3-shNC, PC3-shMETTL3-1/2, LNCaP-vector and LNCaP-METTL3 group. For intratibia injection, 1×10^6 cells were injected into the cortex of the right tibia. The presence of tumor in bone was examined by localization of X-ray imaging. After 8 weeks observed, the mice were sacrificed, and the tumors were dissected for HE stain.

Statistical analysis

Each experiment was in triplicate in parallel. Data were presented as the Mean ± Standard Deviation. The differences among groups were analyzed using one-way analysis of variance. All the statistical analyses were performed using

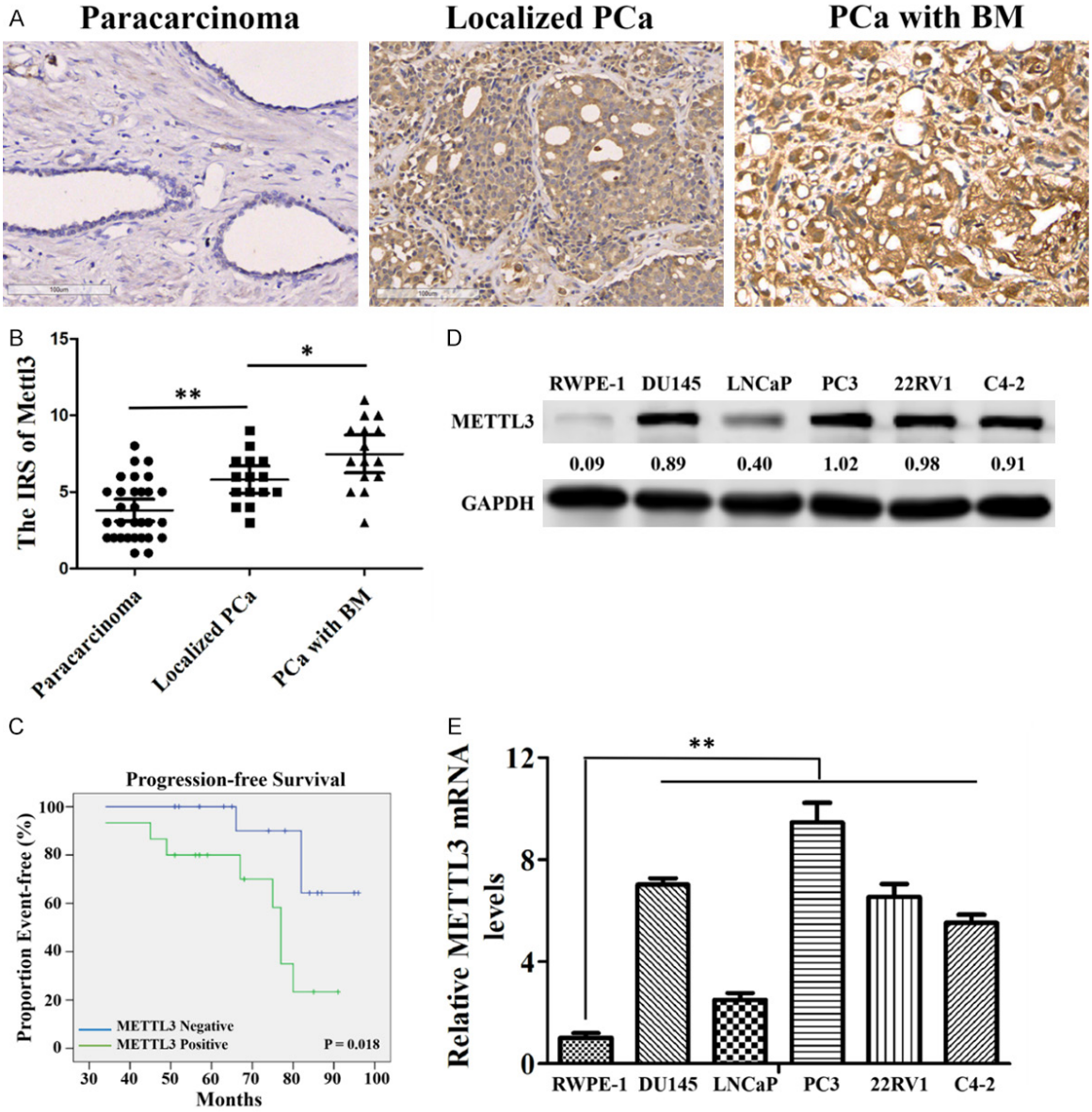

Figure 1. METTL3 expression is positively correlated with the risk of bone-specific metastasis in PCa. A. Immunohistochemical analysis of METTL3 in prostate carcinoma and pericarcinous tissue; B. The IRS of METTL3 in each group; C. Kaplan-Meier survival curves of OS. Lower METTL3 expressions were significantly correlated with longer OS (P=0.018); D, E. The expression of METTL3 in various prostate cells was analyzed by Western Blot and qRT-PCR, GAPDH was used as a loading control. *P < 0.05, **P < 0.01.

the SPSS 18.0 software. *P* values < 0.05 were considered to be statistically significant.

Results

METTL3 is overexpressed in PCa tissues and correlated with PCa BM and OS

Totals of 15 localized PCa tissues, 15 PCa with BM and corresponding adjacent tissues were analyzed for METTL3 protein expression using immunohistochemistry. METTL3 antibody stained cytoplasm and nucleus and gave evenly distributed staining pattern with various intensities (**Figure 1A**). METTL3 expression was present in 28 of 30 (93.3%) cases and 14 of 30 (46.7%) cases for PCa tissues and paracarcinoma, respectively. Mean METTL3 staining intensity was significantly higher in PCa tissues compared with paracarcinoma (5.80 ± 1.61 versus 3.80 ± 1.92, P = 0.002, **Figure 1B**), especially the expression levels of METTL3 were highest in PCa with BM (7.47 ± 2.23, P =

Table 1. The expression pattern of METTL3 in PCa and adjacent non-cancerous prostate tissues by using immunohistochemical staining

Intensities	PCa with BM	Localized PCa	Paracarcinoma
Strong n (%)	3 (20.0)	0	0
Moderate n (%)	7 (46.7)	5 (33.3)	4 (13.3)
Weak n (%)	4 (26.7)	9 (60.0)	10 (33.3)
Undetectable n (%)	1 (6.6)	1 (6.7)	16 (53.3)
Total	15	15	30

0.026 VS localized PCa). The detail IRS of METTL3 in each group was shown in **Table 1**. The associations of METTL3 expression with OS of PCa patients were analyzed using Kaplan-Meier survival analysis (**Figure 1C**). Lower METTL3 expression were significantly correlated with longer overall survival in patients with PCa (P = 0.018, respectively). We also quantify METTL3 expression pattern in normal prostate epithelial cells RWPE-1 and five PCa cell lines by Western blotting (**Figure 1D**) and qRT-PCR (**Figure 1E**). METTL3 expression in RWPE-1 cells was considered baseline, it was found that the METTL3 was highly expressed in PCa cells, especially in PC3. In five tumor cell lines, METTL3 expression in LNCaP cells was relatively lower expressed, so PC3 and LNCaP were selected to perform the experiments.

METTL3 increases adhesion of PCa cells to Collagen I and PCa motility

We first constructed a lentiviral vector expressing METTL3 and shMETTL3 sequence, and established stable cell lines LNCAP-METTL3 and PC3-shMETTL3 after lentivectors transduction. qRT-PCR analysis confirmed that the silencing effect of PC3 was up to 70~80%, and the overexpression effect of LNCaP was up to more than 230 times (**Figure 2A**, **2B**). Type I Collagen is the most common bone protein, to which cancer cells bound facilitated the directional metastasis to the skeleton. To assess the role of METTL3 in cell adhesion to Collagen I, the cancer cell-bone matrix adhesion assays were performed. METTL3 increased the ability of LNCaP cells adhesion to Collagen I. Conversely, METTL3 knockdown in PC3 cells had fewer cell binding with Collagen I compared with PC3-NC cells (**Figure 2C**). For other matrix proteins, METTL3-positive and METTL3-silenced cells adhered equally to fibronectin, laminin, and vitronectin (**Figure 2D**). We examined the effect of METTL3 on the migratory abilities of PCa cells. Transwell assay confirmed that the cell migration rate of cells was decreased by METTL3 knock-down (**Figure 2E**). In contrast, the migration of the PCa cells was significantly promoted by METTL3 overexpression. Moreover, the up-regulated expression of METTL3 promoted and the knockdown inhibited PCa cells survival and proliferation in Collagen I-rich environment (**Figure 2F**).

ITGB1 mediates the adhesion ability of PCa cells by METTL3 expression

To investigate the potential mechanism of METTL3-mediated adhesion of PCa cells to ECM, WB and qRT-PCR were performed to detect the related adhesion molecules, which facilitate cancer cell migration and attachment to the bone. Transfection of LNCaP cells with the METTL3-expressing vector increased ITGB1 expression, whereas transfection of PC3 cells with METTL3 shRNA markedly inhibited ITGB1 expression (**Figure 3A**). Expression levels of the PCa bone metastasis-associated markers, integrin α2, αv, β3 were unaffected (**Figure 3B**). Consistent with our findings, ITGB1 showed a significant positive correlation, with METTL3 in expression across PCa patient samples (n = 98) from TCGA (Gulzar et al., 2012) in GSE40272 dataset from the Genotype-Tissue Expression Project (GTEx). ITGB1 is the most common cell surface receptors for Collagen I. We transfected LNCaP-METTL3 cells with two siRNA sequences to silence ITGB1 expression (**Figure 3C**), the results showed that ITGB1 silence inhibited the METTL3-enhanced binding to Collagen I and invasion in LNCaP-METTL3 cells (**Figure 3D**, **3E**). Furthermore, the effects seen in vitro on tumor cell adherence and migration could also be blocked by blocking antibodies to ITGB1, and not to other integrins (**Figure 3F**, **3G**). Therefore, METTL3 facilitated PCa cells recruitment to Collagen I by increasing ITGB1 expression levels.

METTL3 regulated ITGB1 expression in an m6A-dependent manner

In the study, the results showed that METTL3-positive PCa cells prefered to adhere to Collagen I by upregulating ITGB1 expression compared with METTL3-silenced PCa cells. Then,

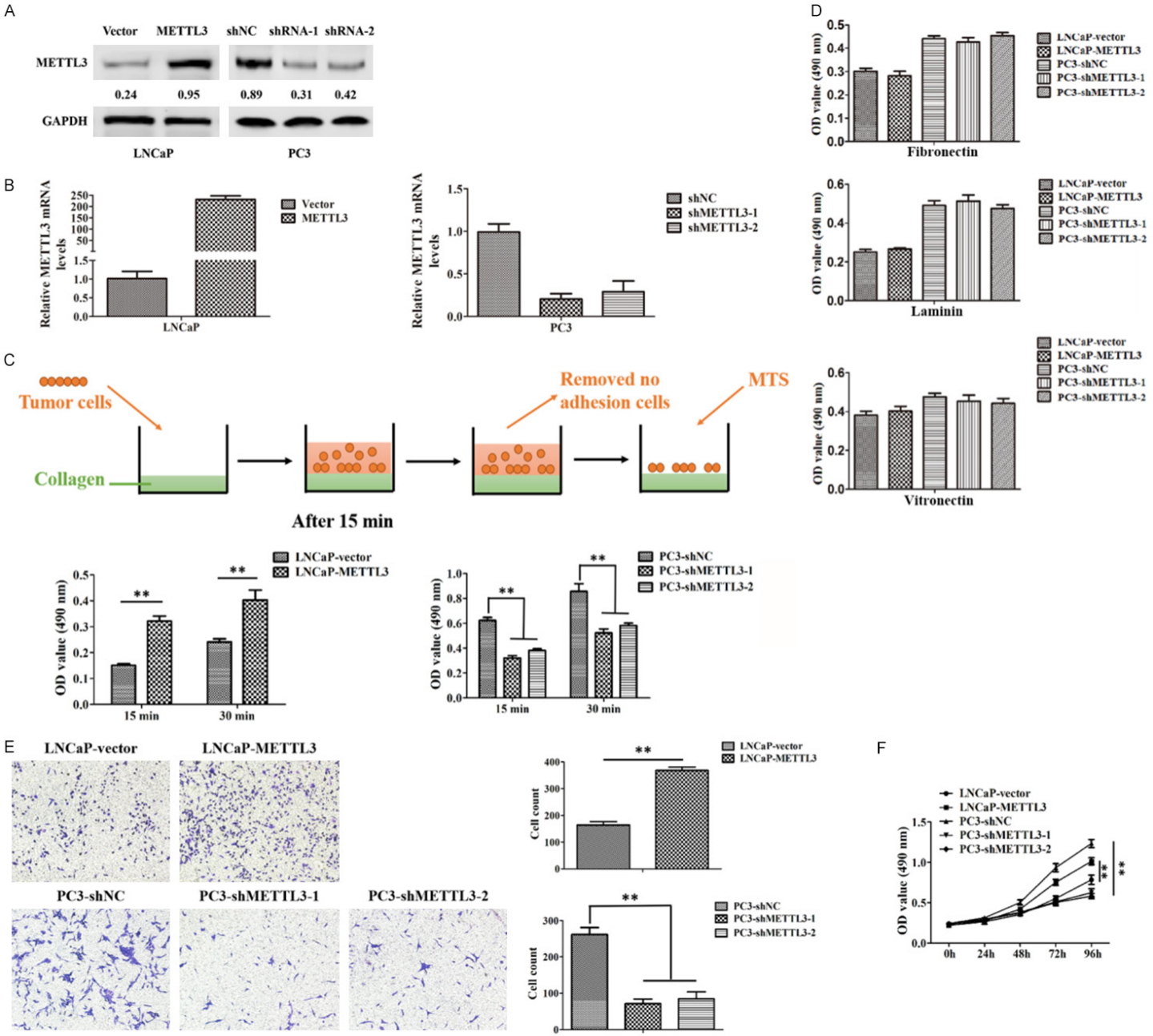
A
Vector
METTL3
shNC
shRNA-1
shRNA-2
METTL3
0.24
0.95
0.89
0.31
0.42
GAPDH
LNCaP
PC3
B
Relative METTL3 mRNA levels
Vector
METTL3
LNCaP
shNC
shMETTL3-1
shMETTL3-2
PC3
C
Tumor cells
Collagen
Removed no adhesion cells
MTS
After 15 min
OD value (490 nm)
LNCaP-vector
LNCaP-METTL3
15 min
30 min
PC3-shNC
PC3-shMETTL3-1
PC3-shMETTL3-2
D
Fibronectin
Laminin
Vitronectin
E
LNCaP-vector
LNCaP-METTL3
PC3-shNC
PC3-shMETTL3-1
PC3-shMETTL3-2
Cell count
F
OD value (490 nm)
0h
24h
48h
72h
96h

Figure 2. Effects of METTL3 on the PCa cells adhesion and motility. Successful construction of stable knockdown or up-regulated PCa cell lines. A, B. The expression level of METTL3 in stable cell lines was analyzed by Western Blot and qRT-PCR; C. Assays to assess the adhesion of cancer cells to the bone matrix Collagen I; D. Assays to assess the adhesion of cancer cells to other matrix proteins; E. The migration ability of cancer cells was assessed by transwell assay; F. METTL3 overexpression promoted, while knockdown inhibited PCa cells survival and proliferation in Collagen I-rich environment. *P < 0.05, **P < 0.01.

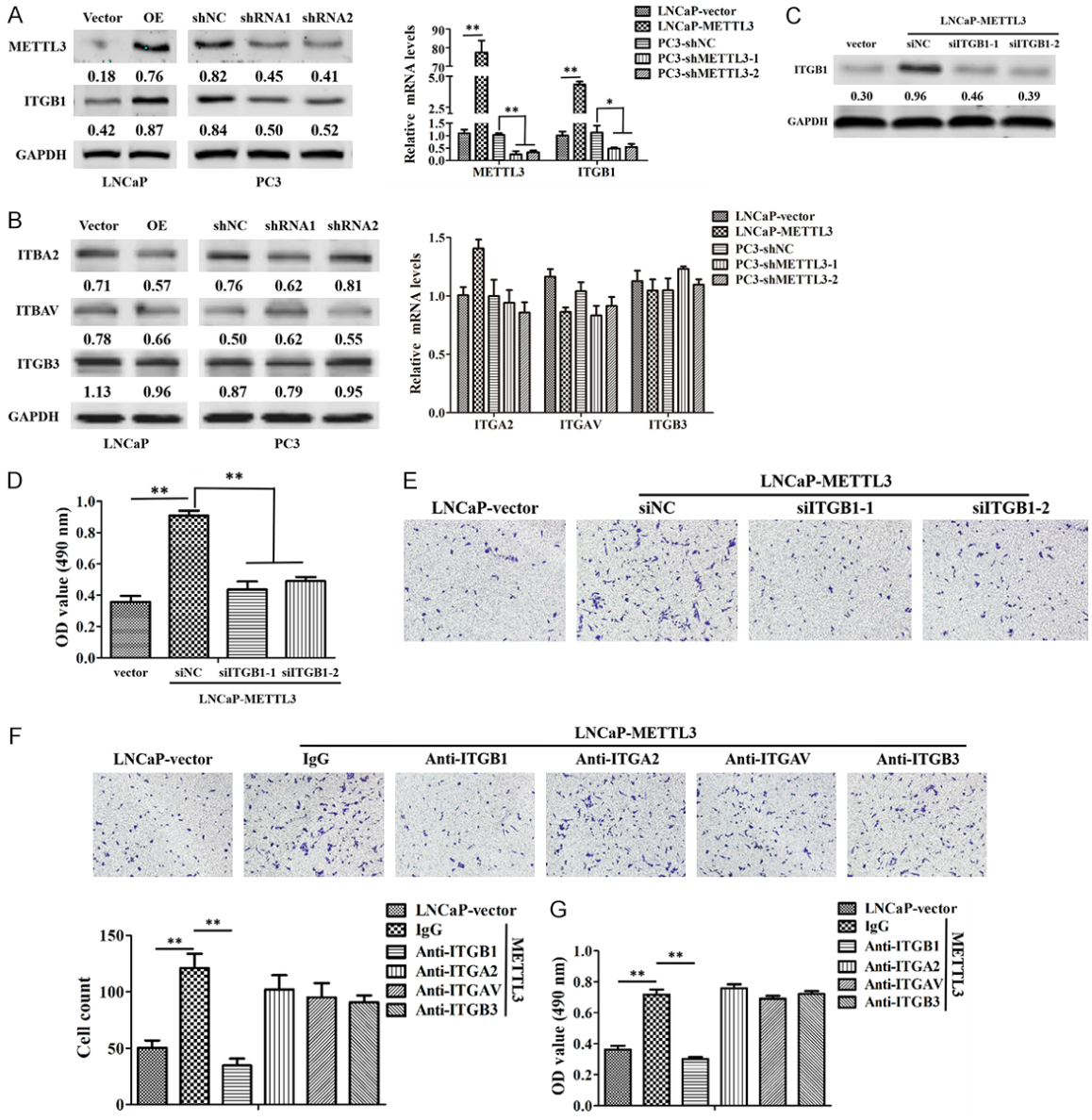

Figure 3. ITGB1 are involved in METTL3-mediated cell adhesion and migration. (A, B) The expression of Integrin in PCa cells, including PC3-NC, PC3-shRNA1, 2; LNCaP-vector, LNCaP-METTL3; (C-E). LNCaP-METTL3 cells were transfected with ITGB1 siRNA1/2 for 24 h, ITGB1 expression were determined by Western blot analyses (C); Adhesion assays showed that ITGB1 silence inhibited the METTL3-enhanced binding to Collagen I in LNCaP-METTL3 cells (D); Transwell assays were used to evaluate the migration abilities of the cells (E); (F, G) After special antibody block integrin, adhesion assays and transwell assays were used to evaluate the adhesion and invasion abilities of the cells. *P < 0.05, **P < 0.01.

we used the protein synthesis inhibitor CHX (cycloheximide) and the proteasome inhibitor MG132 to further study the regulatory mechanism of METTL3 on ITGB1 expression. The results showed that CHX, but not MG132, significantly abolished METTL3 knockdown-in-

duced downregulation of ITGB1 protein expression in PC3 cells, suggesting that METTL3 seems to regulates ITGB1 protein synthesis by modulating the stability and/or translation of ITGB1 mRNA (**Figure 4A**). m6A dot blots assay also demonstrated that knockdown of endogenous METTL3 by shRNAs in PC3 cells decreased global m6A levels (**Figure 4B**). The m6A level changes of ITGB1 mRNA transcripts was assessed by gene-specific m6A qPCR, the results showed that PC3 transfected with METTL3 shRNA sequence contain much lower levels of m6A compared to those with scramble sequence (**Figre 4C**). To determine whether ITGB1 is a direct target of METTL3, we performed luciferase reporter assays. Luciferase activity was decreased in PC3-shMETTL3 cells by transfecting with the reporter construct carrying wild-type ITGB1 3'UTR and CDS compared with PC3-shNC cells; this decrease was abrogated when the putative m6A sites (m6A was replaced with T) were mutated (**Figure 4D**). As expected, forced expression of wild-type METTL3 increase m6A levels of ITGB1 mRNA, enhanced luciferase activity of the reporter construct carrying wild-type ITGB1 3'UTR and CDS, but not mutant m6A sites, relative to the control (**Figure 4E**). To explore the biological function of METTL3-mediated m6A modification in ITGB1 mRNA metabolism, actinomycin D (A9415, Sigma-Aldrich) was added to PCa cells at 5 mg/ml to assess RNA stability. Knockdown of METTL3 decreased, while METTL3 overexpression improved the mRNA stability of ITGB1 (**Figure 4F**, **4G**). Taken together, our results demonstrated that the modulation of ITGB1 expression was under the control of METTL3-associated m6A modification.

HuR enhances ITGB1 mRNA stability via an m6A-dependent manner

The diversity mRNA fate is determined by specific m6A-binding proteins, for example, YTHDF2 mediates mRNA degradation by binding m6A-modified mRNA, thus accurately regulating gene expression at the mRNA level [18]. Conversely, YTHDF1 promotes the binding of m6A-mRNA to the ribosome, which facilitates the translation of RNA [19]. Interestingly, knockdown of HuR, but not the YTH family, decreased the mRNA stability of ITGB1 (**Figure 5A**, **5B**). RIP assays also validated the interaction between the HuR and ITGB1 mRNA in PC3 and LNCaP cells (**Figre 5C**). Consistently, HuR was overexpressed in PCa tissues and widely expressed in multiple PCa cell lines (**Figure 5D**). Knockdown of HuR decreased, while forced overexpression of HuR increased, ITGB1 protein and mRNA expression, the adhesion ability of PCa cells to collagen I, cell migration in tumor cells in vitro (**Figure 5E-G**). Additionally, the direct interaction between HuR and ITGB1 transcripts was impaired in PC3 cells after METTL3 inhibition (**Figure 5H**). These findings indicate that HuR-mediated mRNA stability controls the expression of the ITGB1 in PCa cells via an METTL3-m6A-dependent mechanism.

METTL3 knockdown represses bone metastasis of PCa cells in vivo

To investigate the effect of METTL3 on the bone metastasis of PCa in vivo, we injected PC3-shMETTL3-1/2 cells, LNCaP-METTL3 cells and its corresponding control group cells in the tibiae of mouse models. At 8 weeks after injection, mice were sacrificed. As observed with the use of HE staining, tumor cells caused bone absorption and bone destruction (**Figure 6B**). Furthermore, the localization of tumor in bone was corroborated by X-ray imaging. Representative image of mice inoculated with cells expressing each construct is shown in **Figure 6A**. There were 4 mice demonstrated tumor growth in the METTL3-positive PC3-shNC group, however, only 0~1 of 4 mice was observed in the METTL3-silenced PC3-shMETTL3-1/2 group. In contrast, no tumor growth was observed to having tumors in the bones of LNCaP-vector group, 2 of 4 LNCaP-METTL3 mice demonstrated tumor growth. Those results suggested that METTL3-positive PCa cells prefer the growth in bones compared with the METTL3-silenced PCa cells in mice models.

Discussion

RNA m6A modification exert diverse biological functions in mammals, such as transcription splicing, nuclear RNA export, protein translation control, and cell fate determination at post-transcriptional level [7]. A growing number of studies have found that the abnormal expression of m6A methyltransferase, demethylase and reader proteins were closely related to the occurrence of cancer [20-22]. However, few studies directly focus on the role of m6A modification in PCa. In this study, we examined the

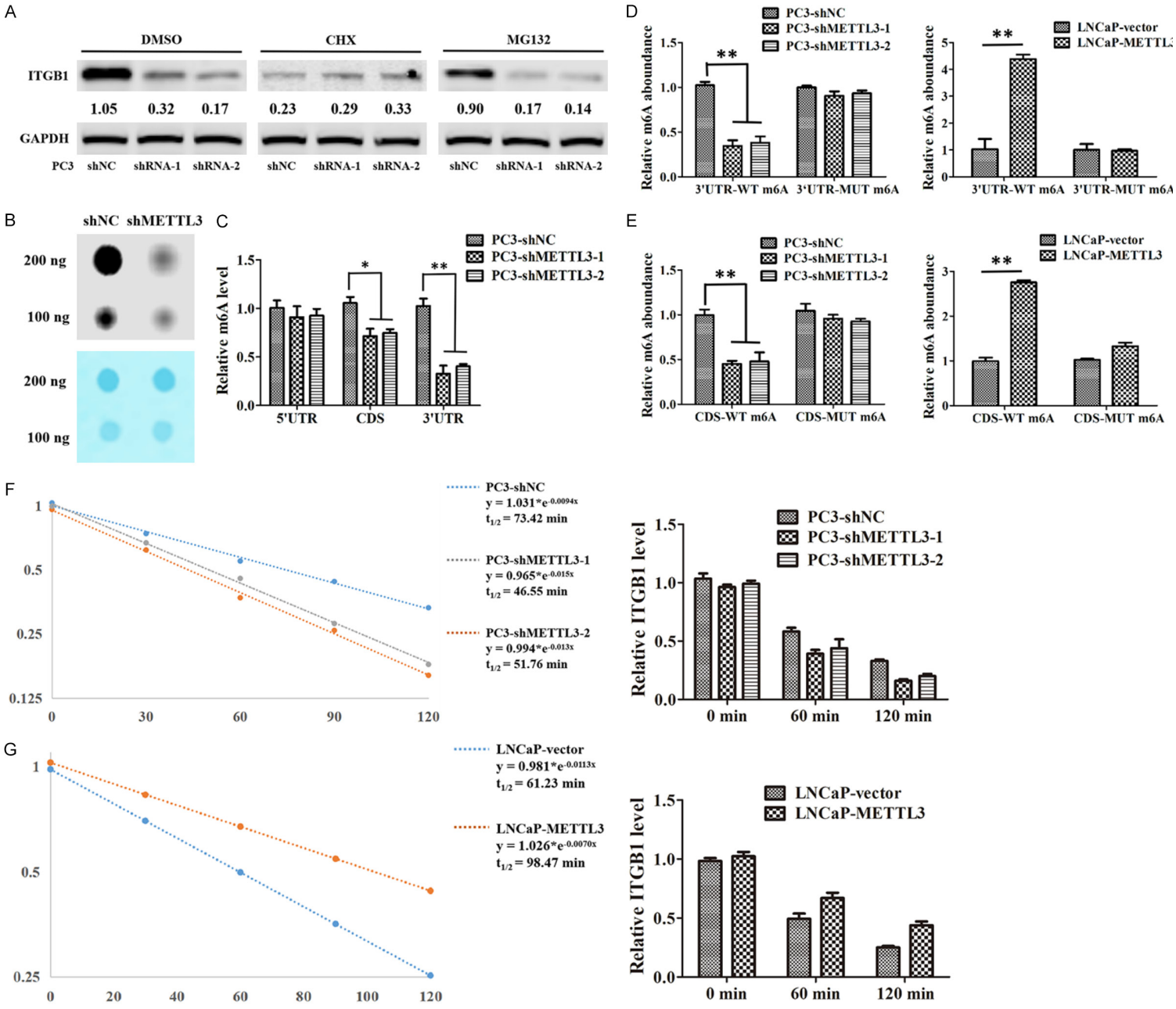
A
DMSO
CHX
MG132
ITGB1
1.05 0.32 0.17 0.23 0.29 0.33 0.90 0.17 0.14
GAPDH
PC3 shNC shRNA-1 shRNA-2 shNC shRNA-1 shRNA-2 shNC shRNA-1 shRNA-2
B
shNC shMETTL3
200 ng
100 ng
200 ng
100 ng
C
PC3-shNC
PC3-shMETTL3-1
PC3-shMETTL3-2
Relative m6A level
5'UTR CDS 3'UTR
D
PC3-shNC
PC3-shMETTL3-1
PC3-shMETTL3-2
Relative m6A aboundance
3'UTR-WT m6A 3'UTR-MUT m6A
LNCaP-vector
LNCaP-METTL3
E
CDS-WT m6A CDS-MUT m6A
F
PC3-shNC
y = 1.031*e-0.0094x
t1/2 = 73.42 min
PC3-shMETTL3-1
y = 0.965*e-0.015x
t1/2 = 46.55 min
PC3-shMETTL3-2
y = 0.994*e-0.013x
t1/2 = 51.76 min
Relative ITGB1 level
0 min 60 min 120 min
G
LNCaP-vector
y = 0.981*e-0.0113x
t1/2 = 61.23 min
LNCaP-METTL3
y = 1.026*e-0.0070x
t1/2 = 98.47 min

Figure 4. METTL3 regulated ITGB1 expression in an m6A-dependent manner. A. Cells were treated with 50 μg/ml CHX (cycloheximide), 10 μM MG132 or DMSO for 24 h, followed by detection of ITGB1 protein levels; B. The global m6A levels in PCa were determined by m6A dot blot; C. Gene-specific m6A qPCR validation of m6A level changes of ITGB1 mRNA in PC3 cells; D, E. Luciferase reporter and mutagenesis assays. Each stable cells were co-transfected with ITGB1-CDS or ITGB1-3'UTR bearing wild-type or mutant (m6A replacedby T) m6A motifs; F, G. Effects of METTL3 on ITGB1 mRNA stability. *P < 0.05, **P < 0.01.

expression pattern of METTL3 in PCa tissues, and analyze its relationship with clinical pathology as well as survival rate of patients. We demonstrated that compared with adjacent benign prostatic epithelia, METTL3 protein levels were obviously up-regulated in PCa tissues, especially in patient with bone metastasis. METTL3 knockdown inhibited PCa cell aggression by m6A-dependent translation control in vitro. These results suggested that METTL3 played an oncogen on the progression of PCa, though there are other studies that had suggested some controversial conclusions. Vu et al. stated that METTL3 promotes the translation of c-MYC, BCL2 and PTEN mRNAs in human myeloid leukemia cells, and decreased the levels of apoptosis in leukemia cells [23]. However, METTL3 depletion promotes the growth and self-renewal of glioblastoma stem cells through down-regulating ADAM19 expression [24]. m6A plays a dual role of either as a tumor suppressor, or an oncogene in cancer [25], which seemly depends on various functions of target genes or the specific recognition of m6A-binding proteins that determines the fate of target genes, however, the concrete mechanism need be further elucidated.

Tumor cells present a number of adhesive abnormalities which contribute significantly to their ability to invade locally and at a distance [26]. Alterations in the expression of the integrins and molecules regulating the downstream signaling events they mediated are associated with cancer metastasis [27]. Collagen type I is the most abundant protein within the bone, making up >90% of the total protein within this site. PCa cells are chemotactic toward and bind to Collagen I to form the bone metastases. In addition, Type I Collagen Receptor (α2β1) signaling could increase PCa cells adhesion to Collagen, thus promoting tumor cells anchoring to bone [28]. Furthermore, m6A was found to regulate the integrin signaling pathway [29]. In this study, we found that METTL3 expression levels are associated with the risk of PCa bone metastasis. Mechanistically, METTL3 facilitated PCa cells recruitment to Collagen I by increasing ITGB1 expression levels in a m6A-dependent manner. However, METTL3 did not influence the expression of integrin α2, αV, β3, and the adhesion of PCa cells to matrix proteins fibronectin, laminin, and vitronectin. The findings presented here provide a novel mechanism underlying the PCa osteotropism.

To illuminate the molecular mechanism by which METTL3 promoted tumor metastasis in PCa, we performed a GEO2R analysis using the public GEO microarray data. The gene expression profile dataset GSE40272 was downloaded from. From the enrichment analysis, we focused on the integrin signaling pathway, which was previously reported to be highly correlated with malignancy bone metastasis. We confirmed that ITGB1 was regulated by METTL3 and was modified in the 3'UTR and CDS by METTL3-intermediated m6A methylation as determined by RIP assays and luciferase reporter assay, followed by identification with METTL3 shRNA. Furthermore, We transfected LNCaP-METTL3 cells with ITGB1 siRNA to silence ITGB1 expression, the results showed that ITGB1 depletion inhibited the METTL3-enhanced binding to Collagen I in LNCaP-METTL3 cells. Similarly, the effects of METTL3 seen in vitro on tumor cell adherence and migration could also be blocked by blocking antibodies to ITGB1, and not to other integrins. Therefore, METTL3 facilitated PCa cells recruitment to Collagen I by increasing ITGB1 expression levels functioning as an m6A mediator.

Analogous to DNA methylation, the diversity biological function of m6A depends largely on specific m6A-binding proteins. HuR belongs to embryonic lethal abnormal visual (ELAV) family of RNA binding protein that widely present on many cell types. HuR regulates cancer-related target mRNA stability and protein translation at post-transcriptional level, thereby affecting the biological characteristics of the tumor [30]. HuR is also essential for PCa growth and chemoresistance [31]. Recently, Visvanathan reported that HuR bound more efficiently to m6A-

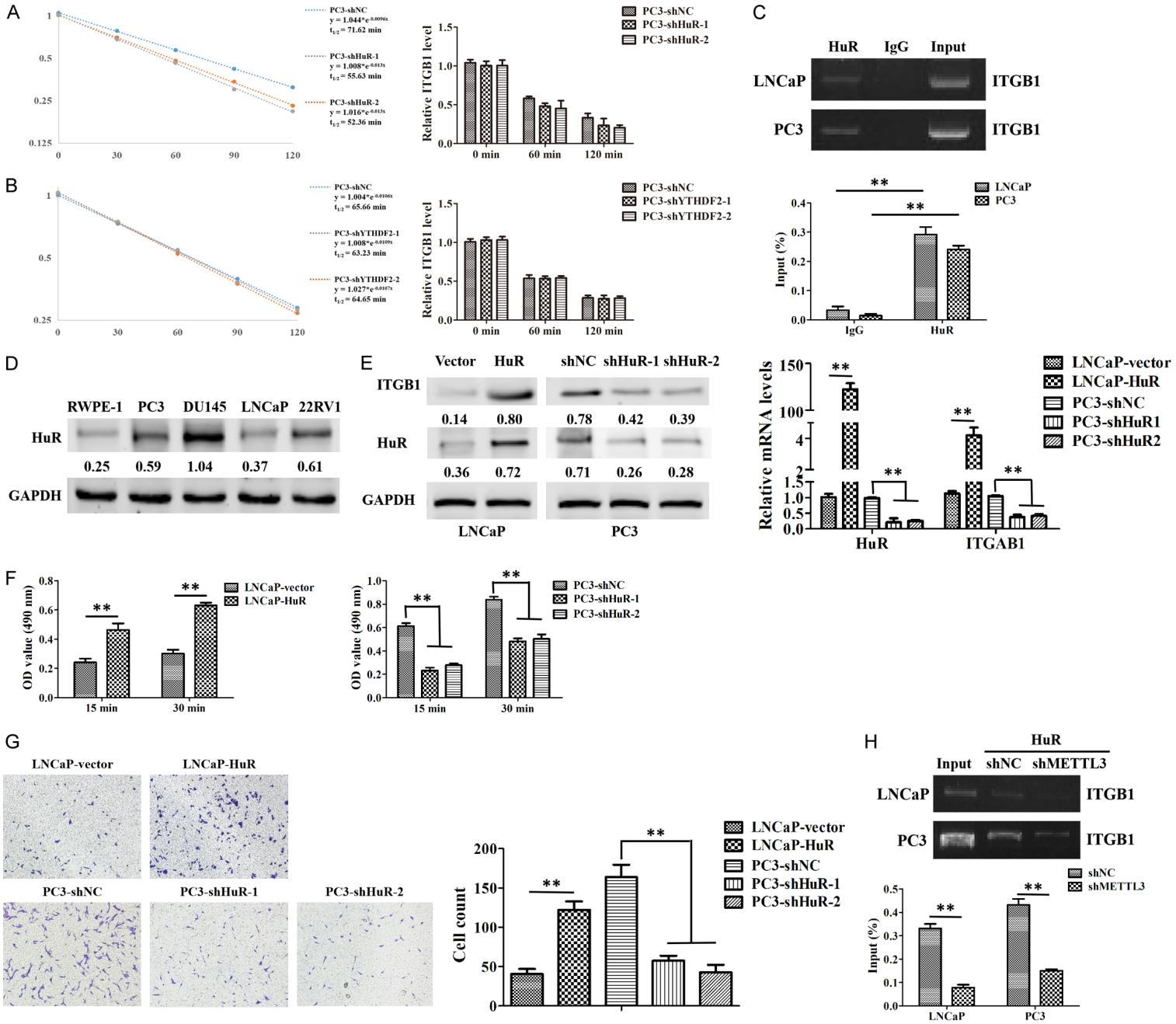
A
PC3-shNC
y = 1.044*e-0.0096x
t1/2 = 71.62 min
PC3-shHuR-1
y = 1.008*e-0.013x
t1/2 = 55.63 min
PC3-shHuR-2
y = 1.016*e-0.013x
t1/2 = 52.36 min
Relative ITGB1 level
0 min
60 min
120 min
B
PC3-shNC
y = 1.004*e-0.0106x
t1/2 = 65.66 min
PC3-shYTHDF2-1
y = 1.008*e-0.0109x
t1/2 = 63.23 min
PC3-shYTHDF2-2
y = 1.027*e-0.0107x
t1/2 = 64.65 min
C
HuR
IgG
Input
LNCaP
PC3
ITGB1
Input (%)
D
RWPE-1
PC3
DU145
LNCaP
22RV1
HuR
0.25
0.59
1.04
0.37
0.61
GAPDH
E
Vector
HuR
shNC
shHuR-1
shHuR-2
ITGB1
0.14
0.80
0.78
0.42
0.39
HuR
0.36
0.72
0.71
0.26
0.28
GAPDH
LNCaP
PC3
Relative mRNA levels
HuR
ITGAB1
LNCaP-vector
LNCaP-HuR
PC3-shNC
PC3-shHuR1
PC3-shHuR2
F
OD value (490 nm)
15 min
30 min
G
LNCaP-vector
LNCaP-HuR
PC3-shNC
PC3-shHuR-1
PC3-shHuR-2
Cell count
H
Input
shNC
shMETTL3
LNCaP
PC3
ITGB1
Input (%)

Figure 5. HuR enhances ITGB1 mRNA stability via an m6A-dependent manner. A. Effects of HuR on ITGB1 mRNA stability; B. Effects of YTHDF2 on ITGB1 mRNA stability; C. RIP assays validated the direct interaction between the HuR and ITGB1 mRNA in PC3 and LNCaP cells; D. The expression of HuR in various prostate cells was analyzed by Western Blot, GAPDH was used as a loading control. E. Immunoblotting assay of ITGB1 after HuR-knockdown in PC3 cells or HuR-overexpression in LNCaP cells; F, G. The effect of HuR on PCa cell adhesion and migration ability; H. After transfected with METTL3 shRNA, Agarose electrophoresis and PCR analysis of RIP assays in PCa cells showing the change of binding between the HuR protein and ITGB1 mRNA. *P < 0.05, **P < 0.01.

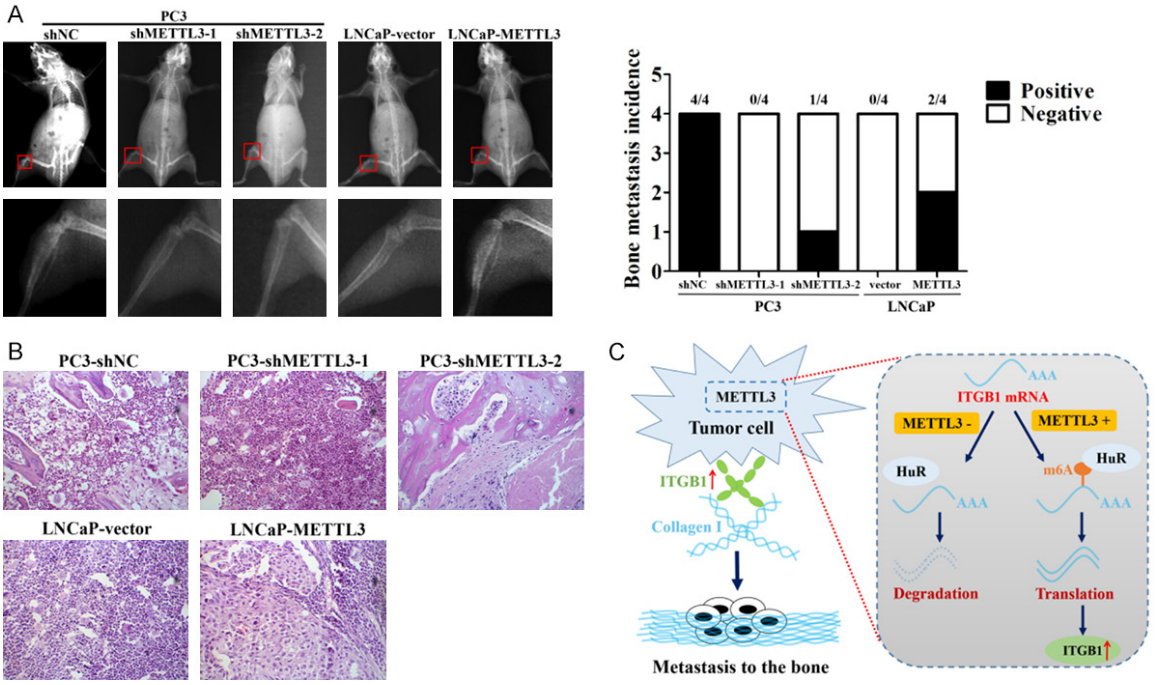

Figure 6. METTL3 promotes bone metastasis of PCa cells in vivo. A. PCa cells were injected in the tibiae of mouse models, and bone destruction were monitored by X-ray imaging; B. H&E analysis for METTL3 of bone metastases from A (mice injected with PCa cells). Magnification, × 200; C. The primary mechanisms by which METTL3-mediated m6A modification promotes bone metastasis of PCa cells.

modified RNA over unmethylated RNA and mediated mRNA stabilization. The recruitment of HuR to m6A-modified RNA is essential for SOX2 mRNA stabilization by METTL3, which mediated glioma stem-like cells maintenance and radioresistance [32]. In this stuy, we also found that HuR was over-expressed in PCa tissues and widely expressed in multiple PCa cell lines. HuR increased its binding to mRNA of ITGB1 because of the increased m6A level, which resulted from METTL3 overexpression, thus increasing the stability of ITGB1 mRNA. This is consistent with the findings of Wu et al., increased HuR levels regulated integrin β1/FAK/ERK signaling, which promoted migration, invasion, and anoikis resistance of metastatic lung cancer cells [33]. However, there are some controversial conclusions. HuR was prone to binding with less m6A-modified RNA and stabilizing its bound counterparts, METTL3 and METTL14 methylated developmental-related RNA and m6A methylation blocked HuR binding, resulting in transcript destabilization. Knockdown of METTL3 or METTL14 reduced m6A to increase HuR-mRNA interaction and prevent miRNA binding [34]. These controversial results may underscore the complicated character of HuR in m6A-modulation which requires further illustrations.

In conclusion, the results of this study provide direct evidence for the modulation of METTL3-positive PCa cells osteotropism. Mechanistically, METTL3 enhances the expression levels of ITGB1 and the adhesion to bone marrow matrix Collagen I in PCa cells, at least partially through HuR-mediated mRNA stability (**Figure 6C**). Our results provide the new therapeutic targets for PCa bone metastasis.

Disclosure of conflict of interest

None.

Address correspondence to: Ran Kang, Department of Urology, The First Affiliated Hospital of University of South China, Hengyang 421001, Hunan, China. Tel: +86-0734-8578599; Fax: +86-0734-8578599; E-mail: rkdr2015@163.com

References

[1] Siegel RL, Miller KD and Jemal A. Cancer statistics, 2019. CA Cancer J Clin 2019; 69: 7-34.
[2] Jin JK, Dayyani F and Gallick GE. Steps in prostate cancer progression that lead to bone metastasis. Int J Cancer 2011; 128: 2545-61.
[3] Rucci N and Angelucci A. Prostate cancer and bone: the elective affinities. Biomed Res Int 2014; 2014: 167035.
[4] Klaassen Z, Howard LE, de Hoedt A, Amling CL, Aronson WJ, Cooperberg MR, Kane CJ, Terris MK and Freedland SJ. Factors predicting skeletal-related events in patients with bone metastatic castration-resistant prostate cancer. Cancer 2017; 123: 1528-1535.
[5] Maden BE. The numerous modified nucleotides in eukaryotic ribosomal RNA. Prog Nucleic Acid Res Mol Biol 1990; 39: 241-303.
[6] Wang X, Lu Z, Gomez A, Hon GC, Yue Y, Han D, Fu Y, Parisien M, Dai Q, Jia G, Ren B, Pan T and He C. N6-methyladenosine-dependent regulation of messenger RNA stability. Nature 2014; 505: 117-20.
[7] Agris PF, Vendeix FA and Graham WD. tRNA's wobble decoding of the genome: 40 years of modification. J Mol Biol 2007; 366: 1-13.
[8] Pan Y, Ma P, Liu Y, Li W and Shu Y. Multiple functions of m6A RNA methylation in cancer. J Hematol Oncol 2018; 11: 48.
[9] Geuens T, Bouhy D and Timmerman V. The hnRNP family: insights into their role in health and disease. Hum Genet 2016; 135: 851-67.
[10] Dai D, Wang H, Zhu L, Jin H and Wang X. N6-methyladenosine links RNA metabolism to cancer progression. Cell Death Dis 2018; 9: 124.
[11] Wang X, Zhao BS, Roundtree IA, Lu Z, Han D, Ma H, Weng X, Chen K, Shi H and He C. N(6)-methyladenosine modulates messenger RNA translation efficiency. Cell 2015; 161: 1388-99.
[12] Roignant JY and Soller M. m6A in mRNA: an ancient mechanism for fine-tuning gene expression. Trends Genet 2017; 33: 380-390.
[13] Su R, Dong L, Li C, Nachtergaele S, Wunderlich M, Qing Y, Deng X, Wang Y, Weng X, Hu C, Yu M, Skibbe J, Dai Q, Zou D, Wu T, Yu K, Weng H, Huang H, Ferchen K, Qin X, Zhang B, Qi J, Sasaki AT, Plas DR, Bradner JE, Wei M, Marcucci G, Jiang X, Mulloy JC, Jin J, He C and Chen J. R-2HG exhibits anti-tumor activity by targeting FTO/m6A/MYC/CEBPA signaling. Cell 2018; 172: 90-105.
[14] Kim H, Yoo JE, Cho JY, Oh BK, Yoon YS, Han HS, Lee HS, Jang JJ, Jeong SH, Kim JW and Park YN. Telomere length, TERT and shelterin complex proteins in hepatocellular carcinomas expressing "stemness"-related markers. J Hepatol 2013; 59: 746-52.
[15] Gieseler F, Ungefroren H, Settmacher U, Hollenberg MD and Kaufmann R. Proteinase-activated receptors (PARs)-focus on receptor-receptor-interactions and their physiological and pathophysiological impact. Cell Commun Signal 2013; 11: 86.
[16] Chen J, Sun Y, Xu X, Wang D, He J, Zhou H, Lu Y, Zeng J, Du F, Gong A and Xu M. YTH domain family 2 orchestrates epithelial-mesenchymal transition/proliferation dichotomy in pancreatic cancer cells. Cell Cycle 2017; 16: 2259-71.
[17] Li E, Liu L, Li F, Luo L, Zhao S, Wang J, Kang R, Luo J and Zhao Z. PSCA promotes prostate cancer proliferation and cell-cycle progression by up-regulating c-Myc. Prostate 2017; 77: 1563-1572.
[18] Wang X, Lu Z, Gomez A, Hon GC, Yue Y, Han D, Fu Y, Parisien M, Dai Q, Jia G, Ren B, Pan T and He C. N6-methyladenosine-dependent regulation of messenger RNA stability. Nature 2014; 505: 117-20.
[19] Wang X, Zhao BS, Roundtree IA, Lu Z, Han D, Ma H, Weng X, Chen K, Shi H and He C. N(6)-methyladenosine modulates messenger RNA translation efficiency. Cell 2015; 161: 1388-99.
[20] Liu J, Yue Y, Han D, Wang X, Fu Y, Zhang L, Jia G, Yu M, Lu Z, Deng X, Dai Q, Chen W and He C. A METTL3-METTL14 complex mediates mammalian nuclear RNA N6-adenosine methylation. Nat Chem Biol 2014; 10: 93-5.
[21] Wang H, Zuo H, Liu J, Wen F, Gao Y, Zhu X, Liu B, Xiao F, Wang W, Huang G, Shen B and Ju Z. Loss of YTHDF2-mediated m6A-dependent mRNA clearance facilitates hematopoietic stem cell regeneration. Cell Res 2018; 28: 1035-1038.
[22] Weng H, Huang H, Wu H, Qin X, Zhao BS, Dong L, Shi H, Skibbe J, Shen C, Hu C, Sheng Y, Wang Y, Wunderlich M, Zhang B, Dore LC, Su R, Deng X, Ferchen K, Li C, Sun M, Lu Z, Jiang X, Marcucci G, Mulloy JC, Yang J, Qian Z, Wei M, He C and Chen J. METTL14 inhibits hematopoietic stem/progenitor differentiation and promotes leukemogenesis via mRNA m6A modification. Cell Stem Cell 2018; 22: 191-205.
[23] Vu LP, Pickering BF, Cheng Y, Zaccara S, Nguyen D, Minuesa G, Chou T, Chow A, Saletore Y,

MacKay M, Schulman J, Famulare C, Patel M, Klimek VM, Garrett-Bakelman FE, Melnick A, Carroll M, Mason CE, Jaffrey SR and Kharas MG. The N6-methyladenosine (m6A)-forming enzyme METTL3 controls myeloid differentiation of normal hematopoietic and leukemia cells. Nat Med 2017; 23: 1369-1376.

[24] Cui Q, Shi H, Ye P, Li L, Qu Q, Sun G, Sun G, Lu Z, Huang Y, Yang CG, Riggs AD, He C and Shi Y. m6A RNA methylation regulates the self-renewal and tumorigenesis of glioblastoma stem cells. Cell Rep 2017; 18: 2622-2634.

[25] Chen XY, Zhang J and Zhu JS. The role of m6A RNA methylation in human cancer. Mol Cancer 2019 29; 18: 103.

[26] Clines GA and Guise TA. Molecular mechanisms and treatment of bone metastasis. Expert Rev Mol Med 2008; 10: e7.

[27] Papachristou DJ, Basdra EK and Papavassiliou AG. Bone metastases: molecular mechanisms and novel therapeutic interventions. Med Res Rev 2012; 32: 611-36.

[28] Hall CL, Dai J, van Golen KL, Keller ET and Long MW. Type I collagen receptor (alpha 2 beta 1) signaling promotes the growth of human prostate cancer cells within the bone. Cancer Res 2006; 66: 8648-54.

[29] Rong ZX, Li Z, He JJ, Liu LY, Ren XX, Gao J, Mu Y, Guan YD, Duan YM, Zhang XP, Zhang DX, Li N, Deng YZ and Sun LQ. Downregulation of fat mass and obesity associated (FTO) promotes the progression of intrahepatic cholangiocarcinoma. Front Oncol 2019; 9: 369.

[30] St Laurent G 3rd, Shtokalo D, Heydarian M, Palyanov A, Babiy D, Zhou J, Kumar A and Urcuqui-Inchima S. Insights from the HuR-interacting transcriptome: ncRNAs, ubiquitin pathways, and patterns of secondary structure dependent RNA interactions. Mol Genet Genomics 2012; 287: 867-79.

[31] Leijon H, Salmenkivi K, Heiskanen I, Hagström J, Louhimo J, Heikkilä P, Ristimäki A, Paavonen T, Metso S, Mäenpää H, Haglund C and Arola J. HuR in pheochromocytomas and paragangliomas - overexpression in verified malignant tumors. APMIS 2016; 124: 757-63.

[32] Visvanathan A, Patil V, Arora A, Hegde AS, Arivazhagan A, Santosh V and Somasundaram K. Essential role of METTL3-mediated m6A modification in glioma stem-like cells maintenance and radioresistance. Oncogene 2018; 37: 522-533.

[33] Wu JI, Lin YP, Tseng CW, Chen HJ and Wang LH. Crabp2 promotes metastasis of lung cancer cells via HuR and integrin β1/FAK/ERK signaling. Sci Rep 2019; 9: 845.

[34] Chen Y, Peng C, Chen J, Chen D, Yang B, He B, Hu W, Zhang Y, Liu H, Dai L, Xie H, Zhou L, Wu J and Zheng S. WTAP facilitates progression of hepatocellular carcinoma via m6A-HuR-dependent epigenetic silencing of ETS1. Mol Cancer 2019; 18: 127.

Table S1. Description of the shRNA sequences

Primer	Sequence
siMETTL3-1	5'-CTGCAAGTATGTTCACTATGA-3'
siMETTL3-2	5'-UCAUAGUGAACAUACUUGCAG-3'
siHuR-1	5'-GCAGCAUUGGUGAAGUUGAAUCU-3'
siHuR-2	5'- GCCCAUCACAGUGAAGUUUGCA-3'
siYTHDF2-1	5'-TTGGCTATTGGGAACGTCCTT-3'
siYTHDF-2	5'-AAGGACGTTCCCAATAGCCAA-3'
siITGB1	5'-AUGGGACACGGGUGAAAAUTT-3'
nonspecific oligos	5'-GCUUCGCGCCGUAGUCUUATT-3'

Table S2A. Description of the primer sequences for PCR

Primer	Sequence
METTL3	
Forward	5'-TTGCGGCCGCAAGGTGTCCGCGTGAGAATTGG-3'
Reverse	5'-GCTCTAGAGCCTTAGCTCTGTAAGGAAGTGCTTC-3'
HuR	
Forward	5'-TTGCGGCCGCAACTTCCCGCCCGTGTTCAGAT-3'
Reverse	5'-CCCTCGAGGGCGTGAGCGAGTTATTTGTGGG-3'

Table S2B. Description of the primer sequences for qRT-PCR

Primer	Sequence
METTL3	
Forward	5'-TTGTCTCCAACCTTCCGTAGT-3'
Reverse	5'-CCAGATCAGAGAGGTGGTGTAG-3'
ITGB1	
Forward	5'-CACGGCTGCTGGTGTTTTCC-3'
Reverse	5'-CCTTCTATTGCTCACCTTGTCC-3'
HuR	
Forward	5'-GGGTGACATCGGGAGAACG-3'
Reverse	5'-CTGAACAGGCTTCGTAACTCAT-3'
ITGA2	
Forward	5'-CCTACAATGTTGGTCTCCCAGA-3'
Reverse	5'-AGTAACCAGTTGCCTTTTGGATT-3'
ITGAV	
Forward	5'-ATCTGTGAGGTCGAAACAGGA-3'
Reverse	5'-TGGAGCATACTCAACAGTCTTTG-3'
ITGB3	
Forward	5'-GTGACCTGAAGGAGAATCTGC-3'
Reverse	5'-CCGGAGTGCAATCCTCTGG-3'
GAPDH	
Forward	5'-CGCTGAGTACGTCGTGGAGTC-3'
Reverse	5'-GCTGATGATCTTGAGGCTGTTGTC-3'